An Octahedral Template Based on a New Molecular Turn: Synthesis and Structure of a Model Complex and a Reactive, Diphenolic Ligand and Its Metal Complexes

Andrew L. Vance,[†] Nathaniel W. Alcock,[‡] Joseph A. Heppert,[†] and Daryle H. Busch*[,†]

Departments of Chemistry, The University of Kansas, Lawrence, Kansas, and University of Warwick, Coventry CV4 7AL, England

Received November 11, 1997

The design and synthesis of a new family of tridentate Schiff base ligands for use in octahedral molecular templates has been successfully demonstrated. As anticipated, two molecules of the ligand, 2,6-pyridinedicarboxaldhydebis-(*p*-hydroxyphenylimine), coordinate equatorially to six-coordinate octahedral metal ions to give orthogonally oriented *molecular turns* around the *anchoring* metal ion. This new template offers the advantages that (1) syntheses of the ligand and its complexes are straightforward, giving high yields in simple, one-pot reactions, and (2) structural variations are easily accomplished. X-ray structural analysis has shown that the ligand will only function as a turn when its spatial organization is controlled by coordination to a metal ion. Upon chelation, the phenolic groups are directed across and beyond the metal ion center, and, unlike earlier ligands of this general type which lacked reactive moieties, substitution reactions may be carried out at the free phenolic groups of the octahedral complex. These reactions remain to be optimized in order to achieve the long-term goal of proving their value as synthons for interlocked molecules.

Introduction

The long-term goal of this work is the creation of a very general molecular template for use as a precursor to supramolecular species.[1] This new molecular template[1] embodies an easily synthesized tridentate Schiff base (structure **1**, R^2 = *p*-phenol) which was designed to function as a *molecular turn*[2]

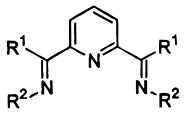

1

by incorporating reactive para-phenolic groups, in a bis-(phenylimine) ligand. Two molecules of this key molecular turn are used in conjunction with a metal ion, which serves as the *anchor,* in a template designed to create a crossover between two turns (structure **2**), a motif often used to create catenanes,

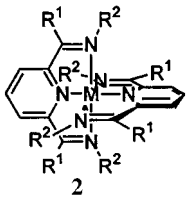

2

rotaxanes, or knots. Two major advantages of this new molecular turn and template are the ease with which the ligands can be synthesized and the corresponding facility with which structures may be varied. The disadvantages derive from the fact that the detailed structural features critical to successful application of the new template are not yet understood. In view of its facile synthesis, this new template has the potential of intensifying advances in many areas of supramolecular chemistry, in for example, the formation of various catenanes, rotaxanes, knots, and still more complicated *orderly molecular entanglements.*[1] Because of the potential value of these systems to the broad realm of supramolecular chemistry, it is appropriate to make these new synthons broadly available at this early date.

This template is inspired by and constitutes the octahedral equivalent of Sauvage's famous tetrahedral template,[3] which is based on a tetrahedral copper(I) *anchor* and two molecules of his unique *molecular turn,* 2,9-bis(4-hydroxyphenyl)-1,10-phenanthroline (structure **3**, see above references). Sauvage and

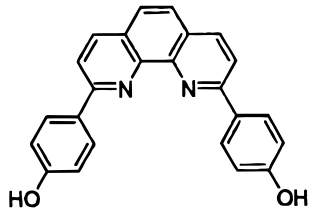

3

Ward have provided a precedent for octahedral templates.[4] They reported the preparation of a catenate using a template based

† The University of Kansas.
‡ University of Warwick.

(1) Busch, D. H. *J. Inclusion Phenom.* **1992**, *12*, 389. Busch, D. H. Ligand Design for Enhanced Molecular Organization—Selectivity and Specific Sequencing in Multiple Receptor Ligands, and Orderly Molecular Entanglements. In *Transition Metal Ions in Supramolecular Chemistry*; Fabbrizzi, L., Ed.; Kluwer: Dordrecht, 1994; pp 55−79.
(2) Busch, D. H.; Vance, A. L.; Kolchinski, A. G. In *Comprehensive Supramolecular Chemistry*; Sauvage, J.-P., Hosseini, M. W., Eds.; Pergamon: Oxford, 1996; Vol. 9, pp 1−42.
(3) (a) Sauvage, J.-P. *Acc. Chem. Res.* **1990**, *23*, 319. (b) Chambron, J.-C.; Dietrich-Buchecker, C. O.; Heitz, V.; Nierengarten, J.-F.; Sauvage, J.-P.; Pascard, C.; Guilhem, J. *Pure Appl. Chem.* **1995**, *67*, 233. (c) Chambron, J.-C.; Dietrich-Buchecker, C.; Sauvage, J.-P. In *Comprehensive Supramolecular Chemistry*; Sauvage, J.-P., Hosseini, M. W., Eds.; Pergamon: Oxford, 1996; Vol. 9, pp 43−84.
(4) Sauvage, J.-P.; Ward, M. *Inorg. Chem.* **1991**, *30*, 3869.

10.1021/ic9714201 CCC: $15.00
Published on Web 12/08/1998

Table 1. Previously Reported Complexes[a]

metal ion	R^1	R^2	ref
Co(II), Fe(II), Ni(II)	H	NH_2	26
Fe(II)	H	Ph	6
Co(II), Co(III)	H	CH_2Ph	6
Cu(II)	H	CH_2Ph	6
Fe(II)	H	OH	6
Co(II), Cu(II), Fe(II),	CH_3	NH_2, $NHCH_3$, NHPh,	27
Ni(II)		$N(CH_3)_2$	
Co(II)	CH_3	2′-NHPy	27
Co(II), Fe(II), Ni(II)	CH_3	CH_3, CH_2CH_3, CH_2Ph, Ph, *p*-ClPh, *p*-FPh, *p*-CH_3Ph, *p*-OCH_3Ph	6
Cd(II), Co(II), Ni(II),	CH_3	Ph, *p*-OCH_3Ph,	10
Zn(II)		*p*-FPh, CH_2Ph	
Ni(II)	CH_3	CH_2CH_3, Ph, CH_2Ph, $(CH_2)_3Ph$	12

[a] R^1 and R^2 correspond to substituents in structure **2**.

on octahedral ruthenium(II) and a Sauvage-type tridentate ligand (structure **4**). As is typical of ligands of that class, a demanding multistep procedure is required to synthesize the disubstituted terpyridine.

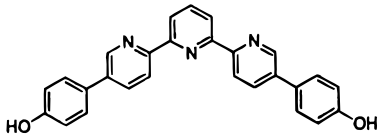

4

Schiff base ligands of general structure **1** have a rich history, beginning with the preparation of the first examples, the pyridinal hydrazones, by Stoufer and Busch,[5] who were motivated by the then current interest in π-back-bonding by unsaturated nitrogen donors. In early work closely related to the systems of interest here, Lions and Martin synthesized Schiff base ligands from 2,6-pyridinedicarboxaldehyde with aniline and benzylamine and noted that the free ligands are crystalline materials.[6] Thereafter, extensive studies ensued in which this same pair of Schiff base linkages were incorporated in many different kinds of polydentate ligands, including various macrocyclic ligands.[7]

Our interest lies in complexes of structure **2** in which the groups R^2 are appropriately functionalized to participate in template reactions. Table 1, which summarizes the previously reported complexes of tridentate Schiff base complexes of this general class, reveals a dearth of ligands having the desired feature.[11] Many of these complexes contain bis(phenylimine) groups derived from aniline or para-substituted anilines; however, none of the para substituents previously reported represent functional groups of convenient reactivity. This is understandable since, in these early studies, interest lay in the effects of these substituents on the metal−ligand bonding.[9−11] Schröder and co-workers recognized the potential for templates of the systems reported here and labeled as a precatenand a ligand which contained an unfunctionalized pendant propyl phenyl group of obvious limited reactivity.[12]

Here we describe the synthesis and characterization of the new ligands, their complexes with metal ions, and the reactivities of the functional groups in these new templates. Initially, the template structure is modeled with a complex which contains unreactive methoxy groups at the para positions of the ligand. That ligand was prepared according to known literature procedures.[9] The crystal structure of the PF_6^- salt of bis[2,6-diacetylpyridinebis(*p*-methoxyphenylimine)]zinc(II) has been determined and is discussed below.

Pursuing the analogy to the Sauvage template, *p*-aminophenol was used as the amine in the straightforward Schiff base condensation reaction with 2,6-pyridinedicarboxaldehyde (PDC) to give the diphenolic ligand. Previous studies on ligands and metal complexes derived from the Schiff bases of *p*-aminophenol are few. In one case, the reaction between PDC and *o*-, *m*-, and *p*-aminophenols in the presence of cadmium ions was used to differentiate aminophenol isomers,[13] and *p*-aminophenol has appeared in some recent publications as a Schiff base precursor. Two of these studies examined hydrogen-bonding interactions of the phenolic hydrogen[14,15] while another involved esterification of the phenolic oxygen of the free Schiff base ligand to construct potential metallomesogen components.[16] Here, we present the preparation and X-ray crystal structure of the free ligand, 2,6-pyridinedicarboxaldhydebis(*p*-hydroxyphenylimine), synthesis of its cobalt(II), iron(II), nickel(II), and zinc(II) complexes, and the reactions of the free phenolic functional groups for some of these compounds. Crystal structures are reported for the free ligand, its zinc(II) and nickel(II) complexes, and the product of methylation of the nickel(II) complex.

Results and Discussion

An Unreactive Model Compound. Recognizing the possibility that phenolic groups may compete with amines and imines for coordination sites, the methylated ligand 2,6-diacetylpyridinebis(*p*-methoxyphenylimine) was chosen to provide a model for the desired coordination behavior. This ligand, L^1, was prepared by Curry's method (Scheme 1),[9] and the cobalt(II), nickel(II), and zinc(II) complexes were prepared. Only the zinc(II) complex is new, and its crystal structure is shown in Figure 1; selected bond angles and distances can be found in Table 2. The geometry of the complex and the spatial arrangement of the ligands are typical for compounds of this class.[12,17]

(5) Stoufer, R. C.; Busch, D. H. *J. Am. Chem. Soc.* **1956**, *78*, 6016.
(6) Lions, F.; Martin, K. V. *J. Am. Chem. Soc.* **1960**, *82*, 2733.
(7) (a) Nelson, S. M. *Pure Appl. Chem.* **1980**, *52*, 2461. (b) Fenton, D. E.; Vigato, P. A. *Chem. Soc. Rev.* **1988**, *17*, 69. (c) Alexander, V. *Chem. Rev.* **1995**, *95*, 273. (d) Guerriero, P.; Tamburini, S.; Vigato, P. A. *Coord. Chem. Rev.* **1995**, *139*, 17.
(8) Parenthetically, the oxime and hydrazine derivatives contain functional groups, but they are deemed too close to the metal ion to be useful in template reactions.
(9) Curry, J. D. Ph.D. dissertation, The Ohio State University, 1964.
(10) Merrell, P. H.; Alyea, E. C.; Ecott, L. *Inorg. Chim. Acta* **1982**, *59*, 25.
(11) Alyea, E. C.; Merrell, P. H. *Inorg. Chim. Acta* **1978**, *28*, 91.
(12) Blake, A. J.; Lavery, A. J.; Hyde, T. I.; Schröder, M. *J. Chem. Soc., Dalton Trans.* **1989**, 965.
(13) Thabet, S. K.; Hagopian, L. *Mikrochim. Ichnoanal. Acta* **1965**, *5−6*, 964.
(14) Yao, W.; Crabtree, R. H. *Inorg. Chem.* **1996**, *35*, 3007.
(15) Aly, M. M.; Imam, S. M. *Monatsh. Chem.* **1995**, *126*, 173.
(16) Nugent, S. J.; Wang, Q. M.; Bruce, D. W. *New J. Chem.* **1996**, *20*, 669.
(17) Lavery, A. J.; Schröder, M. *Acta Crystallogr.* **1996**, *C52*, 37.

Scheme 1

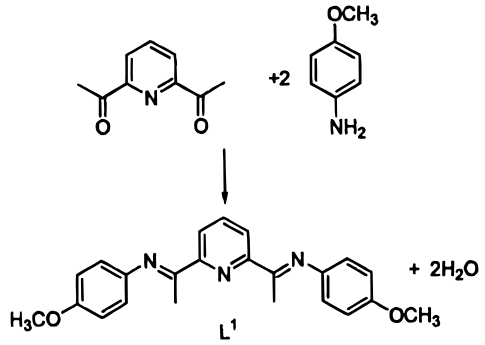

Of primary interest are the positions and intra- and interligand distances of the methoxy oxygens, since this compound represents the structural prototype for the new family of molecular templates based on tridentate, Schiff base ligands. As anticipated, the ligands are meridionally coordinated in a manner which directs the methoxy oxygens accross and beyond the center of the complex. Direct, through-space, intraligand oxygen distances were found to range from 11.424 to 11.727 Å, while interligand oxygen distances were as low as 10.344 Å and as high as 11.493 Å. A more useful measurement of the intraligand oxygen distances would be that which "loops" around the pyridine ring of the opposite ligand, following the path that would be required of a bridging reagent. An approximate value for such a distance was obtained by modeling the addition of a cyano substituent to the para position of the pyridine ring. The cyano nitrogen then occupies the nearest space through which a bridging reagent might pass. By summing the distances from the intraligand methoxy oxygens to the cyano nitrogen, a very approximate "looped" distance of 13.9 Å was obtained. The corresponding intraligand oxygen distances are about 1.6 Å longer than values obtained from a similarly altered Cache molecular model of the tetrahedral Sauvage template (looped distance ca. 12.3 Å), but about 2.8 Å shorter than the looped, intraligand oxygen distances of a Cache model of Sauvage's

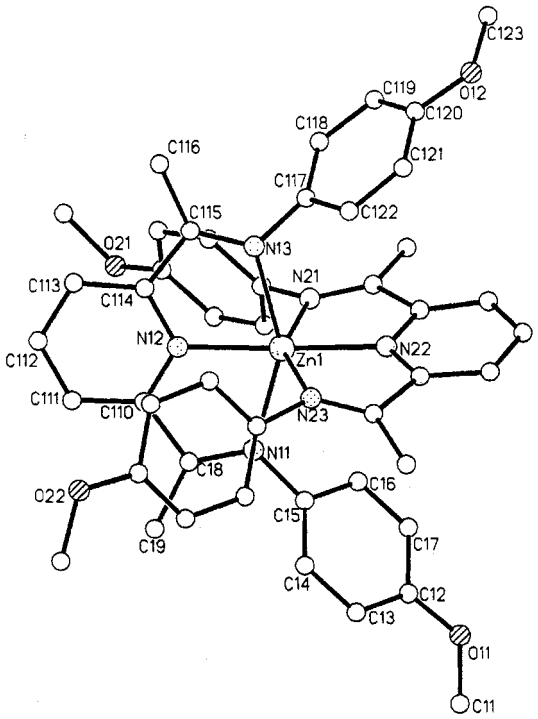

Figure 1. The molecular structure of $Zn(L^1)_2(PF_6)_2$.

Table 2. Selected Bond Lengths (Å) and Angles (deg)

(a) $Zn(L^1)_2(PF_6)_2$

Zn−N(12)	2.034(5)	Zn−N(23)	2.210(6)
Zn−N(22)	2.041(5)	C(115)−N(13)	1.283(9)
Zn−N(21)	2.187(6)	C(18)−N(11)	1.284(8)
Zn−N(13)	2.189(6)	C(215)−N(23)	1.257(8)
Zn−N(11)	2.196(6)	C(28)−N(21)	1.273(8)
N(12)−Zn−N(22)	178.1(2)	N(12)−Zn−N(11)	75.6(2)

(b) L^2

O(1)−O(24)	16.591	C(16)−N(17)	1.276
N(8)−C(9)	1.259	O(24)−O(001)	2.616
N(8)−C(9)−C(10)	121.039	C(12)−C(16)−N(17)	121.431
C(5)−N(8)−C(9)	122.169	C(16)−N(17)−C(18)	120.616

(c) $Zn(L^2)Cl_2$

Zn−N(15)	2.049(7)	Zn−Cl(2)	2.252(3)
Zn−N(8)	2.334(7)	N(8)−C(9)	1.275
Zn−N(17)	2.323(7)	N(17)−C(16)	1.274
Zn−Cl(1)	2.252(3)		
N(15)−Zn−Cl(1)	117.2(2)	N(8)−Zn−N(17)	149.4(3)
N(15)−Zn−Cl(2)	123.5(2)	N(8)−Zn−N(15)	74.8(3)
Cl(1)−Zn−Cl(2)	119.36(10)	N(15)−Zn−N(17)	74.8(3)

(d) $Ni(L^2)_2Cl_2$

Ni(1)−N(215)	1.93(3)	Ni(1)−N(28)	2.21(3)
Ni(1)−N(115)	2.03(2)	N(18)−C(19)	1.39(4)
Ni(1)−N(18)	2.16(3)	N(117)−C(116)	1.29(3)
Ni(1)−N(117)	2.16(3)	N(28)−C(29)	1.24(3)
Ni(1)−N(217)	2.17(3)	N(217)−C(216)	1.15(4)
N(215)−Ni(1)−N(115)	175.5(10)	N(115)−Ni(1)−N(18)	77.6(10)
N(215)−Ni(1)−N(18)	103.0(10)	N(115)−Ni(1)−N(117)	77.4(10)

(e)$Ni(Me-L^2)_2(PF_6)$

Ni(1)−N(142)	1.965(8)	Ni(2)−N(216)	1.960(8)
Ni(1)−N(116)	1.978(8)	Ni(2)−N(218)	2.122(8)
Ni(1)−N(135)	2.180(8)	Ni(2)−N(29)	2.156(9)
Ni(1)−N(118)	2.180(8)	Ni(3)−N(316)	1.983(8)
Ni(1)−N(19)	2.220(8)	Ni(3)−N(318)	2.123(8)
Ni(1)−N(144)	2.233(8)	Ni(3)−N(39)	2.161(8)

N(142)−Ni(1)−N(116)	177.8(3)	N(216)#1−Ni(2)−N(29)	101.1(3)
N(142)−Ni(1)−N(135)	78.5(3)	N(216)−Ni(2)−N(29)	76.7(3)
N(116)−Ni(1)−N(135)	103.7(3)	N(218)#1−Ni(2)−N(29)	101.1(3)
N(142)−Ni(1)−N(118)	103.4(3)	N(218)−Ni(2)−N(29)	154.2(3)
N(116)−Ni(1)−N(118)	76.2(3)	N(216)−Ni(2)−N(29)#1	101.1(3)
N(135)−Ni(1)−N(118)	94.7(3)	N(218)−Ni(2)−N(29)#1	101.1(3)
N(142)−Ni(1)−N(19)	102.5(3)	N(29)−Ni(2)−N(29)#1	84.6(4)
N(116)−Ni(1)−N(19)	77.8(3)	N(316)−Ni(3)−N(316)#2	179.0(5)
N(135)−Ni(1)−N(19)	91.0(3)	N(316)−Ni(3)−N(318)#2	103.0(3)
N(118)−Ni(1)−N(19)	154.1(3)	N(316)−Ni(3)−N(318)	77.7(3)
N(142)−Ni(1)−N(144)	76.3(3)	N(316)#2−Ni(3)−N(318)	103.0(3)
N(116)−Ni(1)−N(144)	101.5(3)	N(318)#2−Ni(3)−N(318)	102.5(5)
N(135)−Ni(1)−N(144)	154.8(3)	N(316)−Ni(3)−N(39)#2	102.3(3)
N(118)−Ni(1)−N(144)	93.0(3)	N(318)−Ni(3)−N(39)#2	83.5(3)
N(19)−Ni(1)−N(144)	92.5(3)	N(316)−Ni(3)−N(39)	77.1(4)
N(216)#1−Ni(2)−N(216)	177.1(5)	N(316)#2−Ni(3)−N(39)	102.3(3)
N(216)−Ni(2)−N(218)#1	104.7(3)	N(318)#2−Ni(3)−N(39)	83.5(3)
N(216)#1−Ni(2)−N(218)	104.7(3)	N(318)−Ni(3)−N(39)	154.8(3)
N(216)−Ni(2)−N(218)	77.5(3)	N(39)#2−Ni(3)−N(39)	101.6(4)
N(218)#1−Ni(2)−N(218)	84.7(4)		

[a] Atom #1 = $-x, y, -z + 1/2$ and atom #2 = $-x + 1, y, -z + 1/2$ from parent atom.

octahedral ruthenium(II) template (looped distance ca. 16.7 Å). Interligand oxygen distances in the model complex (ca. 10.3 Å) are within the range of those for the copper(I) phenanthroline complex (7.8−11.1 Å), but about 4 Å shorter than those of the ruthenium(II) terpyridyl complex (14.1−14.9 Å). From this we conclude that the choice of a bridging ligand of suitable length should both favor catenand formation and circumvent the linking of the ligands together with concomitant formation of a large noninterlocking ring. With information from this model in hand, we switch our focus to the design and synthesis of closely related complexes having reactive functional groups.

A Ligand Having Phenolic Functional Groups. By the general reaction in Scheme 2, diimine molecules, where R is a

Scheme 2

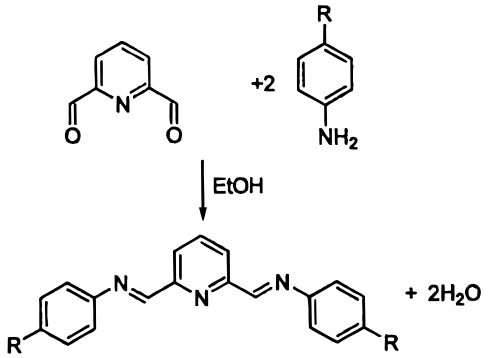

potentially reactive functional group, can be prepared. The most effective method for the isolation of the free ligand was found during an attempt to prepare a nickel(II) complex of 2,6-pyridinedicarboxaldehydebis(*p*-hydroxyphenylimine), L^2. PDC and 2 equiv of *p*-aminophenol were dissolved in warm ethanol to give a yellow solution. While the solution was stirred, a yellow precipitate suddenly appeared. It was collected and found to be nearly pure free ligand in 83% yield. Recrystallization was accomplished from hot ethanol with X-ray quality crystals forming upon cooling to room temperature followed by slow evaporation of the solvent. The X-ray crystal structure (Figure 2) is of interest because it indicates that the preferred conformation of the free ligand is quite unfavorable for either macrocycle formation or chelation. As would be expected, the lone-pair electrons of adjacent nitrogens are directed away from each other such that the molecule is roughly linear. In this configuration, the phenolic oxygens are separated by a distance of 16.591 Å. (Other selected bond distances and angles can be found in Table 2.) Hydrogen bonding was also observed between the phenolic hydrogens and cocrystallized water molecules.

The free ligand, L^2, was the subject of simple experiments to examine the reactivities of those functional groups and of the ligand itself. These are shown in Scheme 3. Reduction of the imine linkages was realized by reaction with sodium borohydride. This particular reaction works especially well since the phenolic groups, which solubilize the ligand as the phenolate in the basic solution of the reaction mixture, also cause the

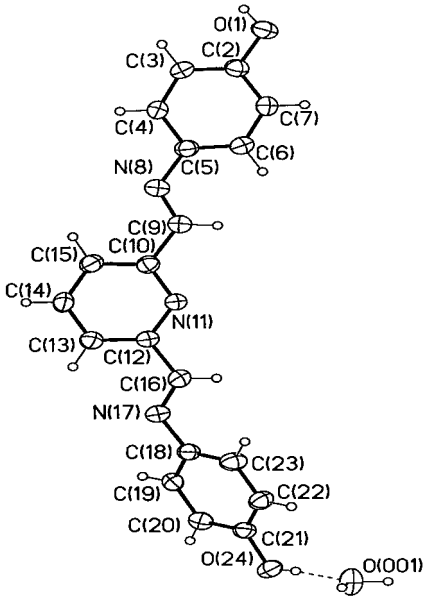

Figure 2. The molecular structure of L^2. Thermal ellipsoids are drawn at the 50% level.

Scheme 3

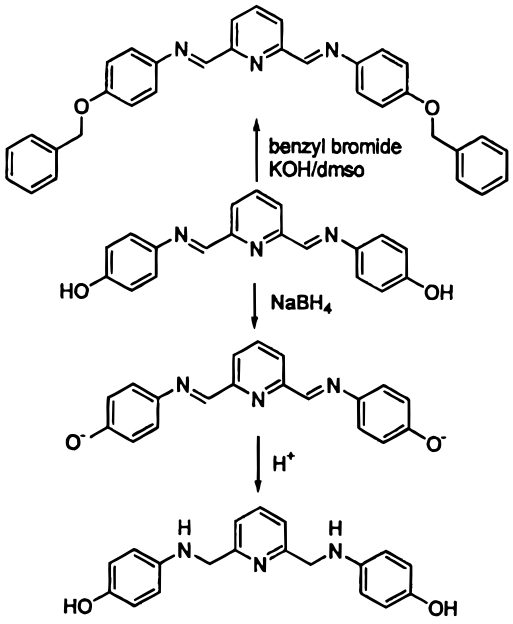

product to precipitate as the neutral diphenol upon neutralization of the solution. In a third reaction the phenolic groups were alkylated by benzyl bromide. It was hoped that the reaction conditions (powdered KOH in DMSO at room temperature) would prove useful for similar alkylation reactions of the transition metal complexes of the ligand. The dibenzylated product was isolated in 54% yield as a microcrystalline powder, and it should be noted that the imine linkages were unaffected by exposure to the DMSO slurry of potassium hydroxide.

Zinc(II) Complex. Attempts to produce the zinc(II) complex of the phenolic ligand, analogous to $Zn(L^1)_2$, gave a yellow precipitate which was found to be soluble only in DMSO And DMF. While its proton NMR spectrum clearly showed the expected resonances of the ligand, other analytical results indicated that the product is not the expected bis complex. The mass spectrum contained only one significant peak, at 416 *m*/*z*, which corresponds to the ion $(ZnL^2Cl)^+$, and the compound was found to be a nonelectrolyte in DMF solution, implying the coordination of the chloride anions. Elemental analysis identified the complex as $Zn(L^2)Cl_2$.

This conclusion was confirmed by X-ray crystallography. Crystals were obtained by very slow (several months) diffusion of toluene into a DMSO solution of the complex. The structure (Figure 3, selected bond lengths and angles in Table 2) shows that the coordination sphere of the zinc is approximately trigonal bipyramidal, a geometry which is not uncommon for halide complexes of zinc(II) containing tridentate ligands.[18,19] This picture nicely highlights the conformational change in the ligand which are expected upon coordination to a metal ion. The diimine ligand is almost planar, unlike the ligand in $Zn(L^1)_2$, presumably due to reduced steric bulk around the metal center. Alyea and co-workers reported the crystal structure of dinitrato-[2,6-diacetylpyridinebis(phenylimine)]nickel(II) in which the phenyl rings of the ligand twist significantly out of the plane of the pyridine.[20] Perhaps the planarity of our ligand can be attributed to the absence of methyl groups at the imine carbon

(18) Lions, F.; Dance, I. G.; Lewis, J. *J. Chem. Soc. A* **1967**, 565.
(19) Furlani, C. *Coord. Chem. Rev.* **1968**, *3*, 141.
(20) Alyea, E. C.; Ferguson, G.; Restivo, R. J. *Inorg. Chem.* **1975**, *14*, 2491.

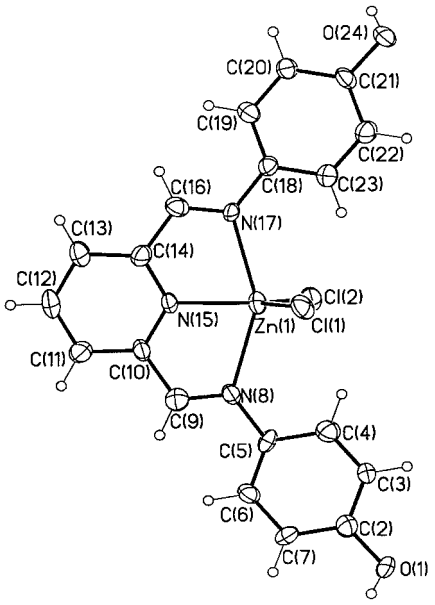

Figure 3. The molecular structure of $Zn(L^2)Cl_2$.

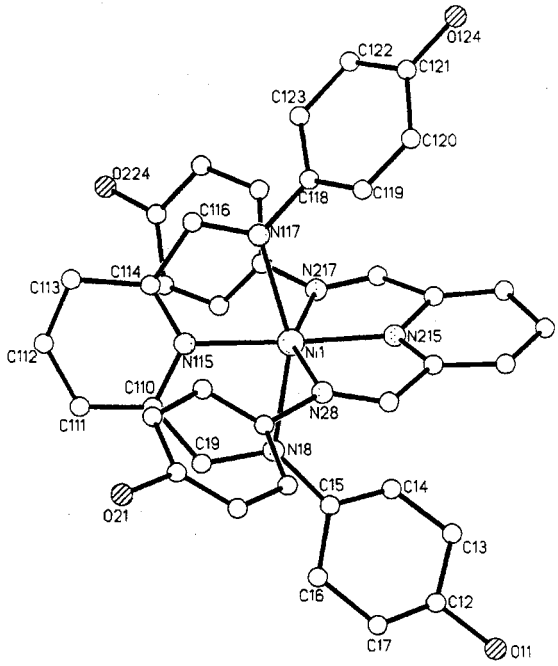

Figure 4. The molecular structure of $Ni(L^2)_2Cl_2$.

which should contribute to the twisting observed by those workers for their diacetylpyridine derivative.

On first glance, ZnL^2 would seem to be an ideal candidate for use as a macrocyclic precursor. Its oxygens are favorably organized for cyclization by an ether formation, such as that utilized by Sauvage and colleagues, and the oxygen separation of 13.14 Å is a distance which could be spanned by a suitably chosen difunctional electrophile. Unfortunately, this is thwarted by the limited solubility of the complex which conspires with an unavoidable tendency to form a totally insoluble, orange precipitate immediately upon exposure to the basic conditions required for ether formation. It is assumed that the phenolate ions bind to vacant zinc sites, producing intractable polymeric structures.

Octahedral Metal Ion Complexes. The nickel(II) complex of L^2 (structure **5**) was successfully isolated and characterized.

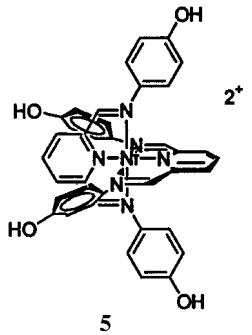

5

The ligand condensation and metal ion complexation reaction are carried out in warm ethanol, and some details are worth noting. First, this reaction should not be presumed to be a template reaction because it has been clearly demonstrated that the ligand is formed in situ by mixing 2,6-pyridinedicarboxaldehyde with *p*-aminophenol. Further, if, even in the presence of the metal ion, stirring is too vigorous or the solution is not warmed sufficiently, the ligand will precipitate. In this case, addition of an ethanolic solution of nickel(II) chloride will still give the desired complex as the ligand redissolves to form the coordination compound, followed by irreversible precipitation of the complex. In any case, the complex is obtained as a red-brown, microcrystalline powder, and recrystallization gives a high yield of X-ray quality crystals.[21]

One reversible Ni^{2+}/Ni^{+} reduction wave was observed in the cyclic voltammogram of the complex with $E_{1/2} = -1.053$ V ($\Delta E_p = 65$ mV) vs ferrocene/ferrocenium. Anion metathesis gave the hexafluorophosphate salt, which is fairly soluble in acetonitrile, and the triflate salt, which is soluble in DMF. Other anions were found to be less useful in improving the solubility or purity of the compound. Cobalt(II) and iron(II) complexes of the phenol-substituted ligand were also prepared, but they proved to be more difficult to purify and were not studied in great depth. The iron(II) complex, which was synthesized under a nitrogen atmosphere, was nearly impossible to purify due to its very poor solubility.

The crystal structure of $Ni(L^2)_2Cl_2$ is shown in Figure 4, and selected bond lengths and angles can be found in Table 2. As expected, the nickel(II) is approximately octahedral, and the ligands are coordinated meridionally to produce the desired orientation of the phenolic oxygens across and away from the center of the complex (as indicated above for the model complex $Zn(L^1)_2(PF_6)_2$). Comparisons can also be made between the monoligated zinc(II) complex of L^2 and the bis complex of

(21) An unusual feature of the complex is its conductivity in water. By standard measurement methods at a concentration of 1.0 mM, the conductance was found to be 173 Ω^{-1} cm^2 mol^{-1}, below the expected range of 235−273 for a 2:1 electrolyte but above the range of 118−131 for a 1:1 electrolyte in water.[22] In view of the composition and crystal structure (discussed below), the compound obviously is a di-univalent electrolyte, so that it must be presumed that the large complex cation must have an unusually low ionic mobility. The problem posed by the unusual conductance is complicated by conductivity measurements at different sample concentrations. Onsager plots of such data (concentration versus conductance) generally produce slopes that correlate with the nature of the electrolyte in question.[23] The observed slope of 325 is higher than typically observed for 2:1 electrolytes in water (anticipated slope ca. 200).[23] Since the phenolic protons are acidic and the acidity may be substantially enhanced by coordination of the ligand to the metal ion, partial ionization of these groups may explain this behavior. However, the high mobility of the proton would lead to the expectation of a large, rather than small, molar conductivity.

(22) Angelici, R. J. *Synthesis and Techniques in Inorganic Chemistry*, 2nd ed.; W. B. Saunders Co.: Philadelphia, 1977; p 213.

(23) Feltham, R. D.; Hayter, R. G. *J. Chem. Soc.* **1964**, 4587.

nickel(II). Whereas the ligand was found to be nearly planar in the zinc complex, the phenyl rings of the two L^2 ligands on nickel(II) are twisted out of the plane of the pyridine rings as was observed for model complex $Zn(L^1)_2$ and other similar complexes.[12,17,20] Steric crowding around the nickel(II) center probably does not allow the ligand to achieve planarity, as it can in the relatively uncrowded ZnL^2Cl_2. In ZnL^2Cl_2, the nearest approach between the phenyl rings is between the interior ortho hydogens, which are 4.50 Å apart. These same hydrogens are separated by about 3.10 Å from the chloride ligands. For the bis complex, $Ni(L^2)_2^{2+}$, a Cache molecular model in which the phenyl rings have been rotated into the plane of the pyridine ring shows that the ortho hydrogen of the phenyl ring more closely approaches the nitrogen of the opposite pyridine. In the crystal structure, this distance is about 2.8 Å, while that distance shrinks to about 2.0−2.3 Å when the phenyl ring is coplanar with the rest of its molecule. Twisting the phenyl rings in the opposite direction, where they are perpendicular to the pyridine plane, creates steric repulsion between ortho hydrogens of opposing ligands. In the crystal structure, these hydrogens are about 2.8 Å removed from each other, but when the phenyl rings are twisted 90° from the plane of the pyridine, that distance is reduced to about 1.5 Å. Clearly, the degree of twisting of the phenyl rings observed in the crystal structure is indicative of the most sterically favorable conformation.

Another difference between the mono and bis complexes is found in the intraligand oxygen distances for $Zn(L^2)^{2+}$ and $Ni(L^2)_2^{2+}$, where "looping" around the second ligand must again be taken into account. The oxygens of the zinc(II) complex are separated by 13.138 Å, while the approximate distance for the nickel(II) complex (determined as described for the methoxy model complex) is 14.6 Å. Interligand oxygen distances from 10.074 to 12.062 Å were determined for $Ni(L^2)_2^{2+}$. These distances bear out expectations from the zinc(II) model complex, $Zn(L^2)^{2+}$, in which the looped intraligand oxygen distance exceeds interligand oxygen distances. As indicated earlier, a similar relationship between intra- and interligand oxygen distances was observed in the Cache models of Sauvage's tetrahedral and octahedral templates.

Reactions of the Nickel(II) Complex. Initial attempts to form the methyl ethers of the four phenol oxygens of the bis complex by reaction of its triflate salt in warm (ca. 55 °C) DMF with cesium carbonate and excess methyl iodide produced only the methylated free ligand (Me-L^2). Apparently, these conditions were harsh enough to demetalate the ligand. Performing the reaction under milder conditions gave more encouraging results. Addition of methyl iodide to the hexafluorophosphate salt of the nickel(II) complex in warm (T < 55 °C), dry acetonitrile, with a stirred suspension of potassium carbonate as the base, gave the tetra-methylated complex in a low, 10% yield. Multiple recrystallizations of the product failed to give analytically pure samples; however, X-ray quality crystals were obtained, and the crystal structure (Figure 5) of the complex is surprisingly similar to that of the unmethylated starting material. While this reaction was clearly far from optimal, it opened the way for the study of the alkylation reactions of the phenol-substituted complex.

Better results were obtained with benzyl bromide as the electrophilic reagent. Mixing the hexafluorophosphate salt of $Ni(L^2)_2$ with a 2-fold excess of benzyl bromide for 24 h at room temperature in an acetonitrile suspension of potassium carbonate gave the tetra-benzylated complex as small, brown needles in 27% yield after recrystallization from acetonitrile/ethanol. In contrast to the tetra-methylated product, this sample was nearly pure according to mass spectral and elemental analytical data. When this same reaction was carried out with stoichiometric quantities of reagents, mass spectral results indicated incomplete reaction. To achieve maximum effectiveness in template reactions using difunctional bridging reagents, the yields need to approach completion even when the reactions are run stoichiometrically. The desired level of optimization of the reaction proved elusive, with respectable yields obtained only when excess electrophile was used.

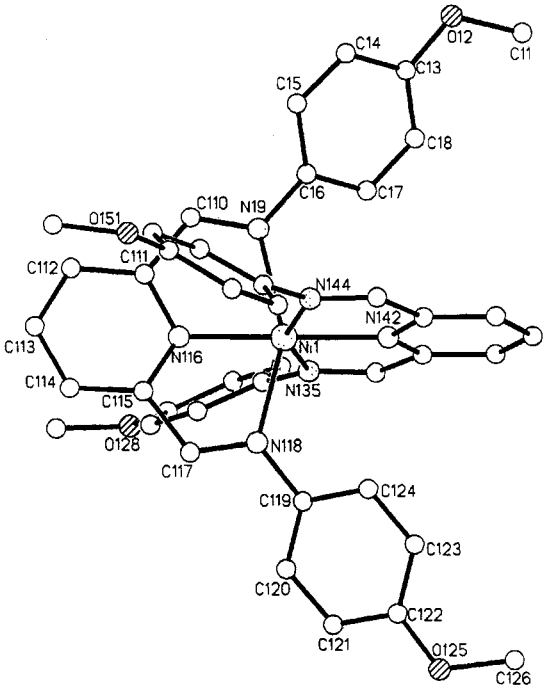

Figure 5. The molecular structure of $Ni(Me\text{-}L^2)_2(PF_6)_2$.

Under various conditions, preliminary experiments directed toward catenate formation using reagents adapted from Sauvage's studies (α,ω-dibromo, -ditosyl, or -diiodo derivatives of hexaethylene glycol) and the nickel(II) complex described here have, so far, yielded tantalizing but inconclusive results. Some difficulties are anticipated in view of the yields of the relatively simple reactions with excess monohaloalkanes. Because of the likelihood of oligomerization, the electrophilic bridging reagent cannot be used in large excess, making it difficult to duplicate the most obvious advantages used in optimizing the reaction conditions for the alkylations with monohaloalkanes. These investigations are ongoing.

Conclusions

The design and synthesis of the first member of a new family of tridentate ligands for use in octahedral molecular templates have been successfully demonstrated. As anticipated, the ligand coordinates equatorially to six-coordinate transition metal ions to give orthogonally oriented molecular turns around the metal ion anchor. The syntheses of the ligand and its complexes proved to be as straightforward as expected, giving high yields of either the free ligand or its complexes in simple, one-pot reactions. X-ray structural analysis has shown that, as anticipated, the ligand will only function as a turn when spatial organization is controlled by coordination to a metal ion. Upon chelation, the phenolic groups are directed across and beyond the metal ion center, and, unlike earlier ligands of this general type which lacked reactive moieties, substitution reactions may be carried out at the free phenolic groups of the octahedral complex. These

reactions must yet be optimized in order to achieve the long-term goal of proving their value as precursors for supramolecular species. This optimization, along with the preparation and study of complexes with different functional groups, represents the focus of ongoing studies.

Experimental Section

Solvents were bulk or reagent grade and used as received unless otherwise noted. Reagents, except where otherwise noted, were purchased from various commercial sources and used as received. Elemental analyses were performed by the analytical service of the Department of Medicinal Chemistry at the University of Kansas. FAB mass spectral measurements were performed by the mass spectrometry lab of the Department of Chemistry at the University of Kansas. Infrared spectra of the samples as KBr pellets were recorded on a Perkin-Elmer 1600 FTIR. Proton NMR spectra were measured on a GE QE300 NMR spectrometer with chemical shifts reported as δ (ppm) relative to the internal solvent standard. The solvent was deuteriochloroform unless otherwise noted. Conductivities were measured with a YSI Scientific model 35 conductance meter. UV/vis absorption spectra were obtained on a model 8452A Hewlett-Packard diode array spectrophotometer. Electrochemical measurements were performed using a Princeton Applied Research model 173 potentiostat fitted with a model 179 digital coulometer and a model 175 universal programmer. Scans were taken at 200 mV/s with a glassy carbon working electrode, silver wire reference electrode, platinum wire secondary electrode, 0.1 M tetrabutylammonium hexafluorophosphate supporting electrolyte, and internal ferrocene standard.

Synthesis of 2,6-Pyridinedicarboxaldehyde. The dialdehyde was prepared by the following modified literature procedure.[24] Activated manganese(IV) dioxide (purchased from Fluka) was prepared for reaction by heating overnight at 110 °C. Excess MnO_2 (100 g) and 10.0 g (71.9 mmol) of 2,6-pyridinedimethanol were refluxed with stirring for 5 h in 500 mL of chloroform (Aldrich spectroscopic grade, used as received). The oxide residue was separated from the solution by vacuum filtration on a fritted glass funnel, and the black residue was rinsed with 4 × 100 mL of chloroform. Solvent was removed from the solution by rotary evaporation, and then the crude product was dissolved in a minimum amount of chloroform and passed through a short (ca. 15 cm long, ca. 4 cm diameter) silica gel column (isocratic elution with chloroform). The pure dialdehyde elutes easily and can be seen as an opaque white band in the clear silica gel while impurities remain at the top of the column. Removal of the solvent by rotary evaporation gives the product in 60−65% yield. Proton NMR spectrum: 10.17 (s, CH, 2H), 8.18 (d, pyH, 2H), 8.08 (t, pyH, 1H) ppm. Mp: 122−123 °C.

Synthesis of 2,6-Diacetylpyridinebis(*p*-methoxyphenylimine), L^1. 2,6-Diacetylpyridine (0.513 g, 3.15 mmol) and *p*-anisidine (0.766 g, 6.22 mmol) were dissolved in 20 mL of methanol with stirring. Several drops of concentrated hydrochloric acid were added, and a beige precipitate appeared from the brown solution. The precipitate was collected by vacuum filtration and dried to give a fluorescent yellow powder in 51% yield. Infrared spectrum: $\nu_{C=N} = 1630$ cm^{-1}. Proton NMR spectrum: 8.3 (d, pyH, 2H), 7.9 (t, pyH, 1H), 6.9 (d, PhH, 4H), 6.8 (d, PhH, 4H), 3.8 (s, OCH_3, 6H), 2.4 (s, CH_3, 6H) ppm. Carbon-13 NMR spectrum: 167.4, 156.4, 155.8, 144.5, 136.7, 122.1, 120.9, 114.5, 55.5, 16.1 ppm.

Synthesis of Bis[2,6-diacetylpyridinebis(*p*-methoxyphenylimine)]-zinc(II) Hexafluorophosphate, $[Zn(L^1)_2](PF_6)_2$. Zinc(II) acetate dihydrate (0.0667 g, 0.304 mmol) was dissolved in 10 mL of methanol with stirring. 2,6-Diacetylpyridinebis(*p*-methoxyphenylimine) (0.205 g, 0.549 mmol) was added to the zinc(II) solution, and stirring was continued for 30 min, giving a clear yellow solution. Filtration of the solution followed by removal of the solvent by rotary evaporation gave a yellow powder. Redissolving the crude product in methanol and filtering into an aqueous solution of ammonium hexafluorophosphate gave a bright yellow precipitate, which was collected by vacuum filtration and rinsed with water and diethyl ether. The crude hexafluorophosphate salt was recrystallized from acetonitrile/ethanol by slow evaporation of the solvents to give yellow crystals in 80% overall yield. Anal. Calcd for $C_{46}H_{46}N_6O_4P_2F_{12}Zn$: C, 50.13; H, 4.21; N, 7.62. Found: C, 50.00; H, 4.48; N, 8.00. Positive ion FAB mass spectrum: *m/z* 956 $(ZnL^1{}_2PF_6)^+$, 810 $(ZnL^1{}_2)^+$. Proton NMR spectrum in CD_3CN: 8.40 (t, pyH, 2H), 8.19 (d, pyH, 4H), 6.70 (d, PhH, 8H), 6.39 (d, PhH, 8H), 3.71 (s, OCH_3, 12H), 2.41 (s, CH_3, 12H) ppm. Infrared spectrum: $\nu_{C=N} = 1628.1$ cm^{-1}.

Synthesis of 2,6-Pyridinedicarboxaldehydebis(*p*-hydroxyphenylimine), L^2. 2,6-Pyridinedicarboxaldehyde (1.00 g, 7.40 mmol) and 4-aminophenol (1.62 g, 14.8 mmol) were stirred in 15 mL of absolute ethanol until a yellow precipitate appeared (within ca. 5 min). Stirring was continued for an additional 30 min, and then the yellow powder was collected by vacuum filtration and dried overnight in a vacuum desiccator. Yield: 83%. Proton NMR spectrum in acetone-d_6: 8.69 (s, OH, 2H), 8.65 (s, CH, 2H), 8.25 (d, pyH, 2H), 8.02 (t, pyH, 1H), 7.35 (d, PhH, 4H), 6.94 (d, PhH, 4H) ppm. Infrared spectrum: $\nu_{O-H} = 3457.1$ cm^{-1} and $\nu_{C=N} = 1617.6$ cm^{-1}. UV/vis spectrum (8.0×10^{-2} mM in methanol): 242 nm ($\epsilon = 2.1 \times 10^4$ cm^{-1} M^{-1}), 294 nm (sh) ($\epsilon = 1.3 \times 10^4$ cm^{-1} M^{-1}), 354 nm (ϵ 2.4 × 10^4 cm^{-1} M^{-1}). Mp: 127−130 °C dec. Dissolving the ligand in hot ethanol followed by slow evaporation of the solvent at room temperature gives yellow, X-ray quality crystals.

Reduction of Azomethines of L^2. 4-Aminophenol (1.16 g, 14.8 mmol) and 2,6-pyridinedicarboxaldehyde (1.00 g, 7.40 mmol) were dissolved in 50 mL of absolute ethanol to give a yellow solution, which was stirred for 1 h. Sodium borohydride in 10-fold excess (1.40 g, 37.0 mmol) was added in portions to the ethanolic solution at 0 °C, and stirring was continued for 20 min. The solution was then refluxed for 30 min. After cooling of the light yellow solution, the ethanol was removed by rotary evaporation. Water (200 mL) was added to give a yellow solution with some precipitate present. Concentrated HCl (ca. 2 mL) was added to neutralize the solution (pH ca. 6−7), causing the color of the solution to lighten and giving an off-white precipitate. After collection of the solid and drying on a Büchner funnel, 2.42 g of product was obtained for an 80% yield. Proton NMR spectrum: 8.43 (s, OH, 2H), 7.64 (t, pyH, 1H), 7.20 (d, pyH, 2H), 6.54 (d, PhH, 4 H), 6.44 (d, PhH, 4H), 5.69 (t, NH, 2H), 4.62 (d, CH_2, 4H) ppm. Infrared spectrum: $\nu_{O-H} = 3406$ cm^{-1}, $\nu_{N-H} = 3297$ cm^{-1}.

Benzylation of L^2. Based on a literature procedure,[25] powdered KOH (0.449 g, 8.00 mmol) was stirred in 2 mL of DMSO for 5 min. L^2 (0.317 g, 1.00 mmol) was added, followed by 0.5 mL of benzyl bromide (0.719 g, 4.20 mmol). The reaction mixture became a slurry so another 1 mL of DMSO was added to completely dissolve L^2 upon continued stirring. After stirring for 60 min, the light yellow mixture was poured into 20 mL of deionized water, followed by extraction with 3 × 20 mL aliquots of methylene chloride. The yellow organic layers were combined and washed with 5 × 10 mL of water. The solution was dried over sodium sulfate and decanted from the drying agent, and the solvent was evaporated by rotary evaporation to give a pale yellow powder, which was dried overnight in a vacuum desiccator. The crude product was recrystallized from hot dichloroethane to give a 54% yield of small, light yellow crystals. Proton NMR spectrum: 8.71 (s, CH, 2H), 8.25 (d, pyH, 2H), 7.90 (t, pyH, 1H), 7.40 (m, PhH, 14H), 7.03 (d, PhH, 4H), 5.11 (s, CH_2, 4H) ppm. Infrared spectrum: $\nu_{C=N} = 1623.7$ cm^{-1}. Mp: 190 °C dec.

Synthesis of $Zn(L^2)Cl_2$. 2,6-Pyridinedicarboxaldehyde (2.00 g, 14.8 mmol) and 4-aminophenol (3.23 g, 29.6 mmol) were dissolved with slow stirring in 30 mL of absolute ethanol. Zinc(II) chloride (2.03 g, 14.8 mmol) was dissolved in 20 mL of ethanol, and its solution was added all at once to the yellow suspension of the free ligand. An orange precipitate appeared immediately and was collected by vacuum filtration. The light orange powder was dried overnight in a vacuum desiccator. Yield: 98%. Anal. Calcd for $C_{19}H_{15}Cl_2N_3O_2Zn$: C, 50.31; H, 3.33; N, 9.26. Found: C, 50.23; H, 3.32; N, 9.40. Proton NMR

(24) Papadopolous, E. P.; Jarrar, A.; Issadorides, C. H. *J. Org. Chem.* **1966**, *31*, 615.
(25) Johnstone, R. A. W.; Roe, M. E. *Tetrahedron* **1979**, *35*, 2169.
(26) Figgins, P. E.; Busch, D. H. *J. Am. Chem. Soc.* **1960**, *82*, 820.
(27) Curry, J. D.; Robinson, M. A.; Busch, D. H. *Inorg. Chem.* **1967**, *6*, 1570.

Table 3. Summary Crystal Data

	$Zn(L^1)_2(PF_6)_2$	L^2	$Zn(L^2)Cl_2$	$Ni(L^2)_2Cl_2$
empirical formula	$[C_{46}H_{46}N_6O_4Zn]\cdot 2[PF_6]$	$C_{19}H_{17}N_3O_3$	$C_{23}H_{27}Cl_2N_3O_4S_2Zn$	$C_{42}H_{42}Cl_2N_6NiO_6S_2$
fw	1102.20	335.36	609.87	920.55
temp/K	220(2)	240(2)	230(2)	200(2)
cryst syst	monoclinic	monoclinic	triclinic	monoclinic
space group	$P2_1/c$	$P2_1/c$	$P\bar{1}$	$C2/c$
a/Å	17.998(11)	11.4073(4)	9.8263(3)	49.46(10)
b/Å	16.832(12)	10.4195(4	11.9415(5)	12.01(3)
c/Å	17.134(13)	13.9444(5)	13.0491(5)	16.20(2)
α/deg	90	90	106.151(2)	90
β/deg	111.69(5)	98.051(2)	94.170(2)	108.10(13)
γ/deg	90	90	114.281(2)	90
vol/Å^3, Z	4823(6), 4	1641.07(10), 4	1309.69(8), 2	9146(32), 8
diffractometer	P3R3	SMART	SMART	P3R3
μ(Mo Kα)/mm^{-1}	0.672	0.094	1.336	0.683
cryst dimens/mm	0.43 × 0.36 × 0.08	0.30 × 0.20 × 0.12	0.20 × 0.04 × 0.04	0.03 × 0.45 × 0.45
θ_{max}	22.60	28.59	23.27	21.04
total reflns	6080	9386	5570	4982
unique, R(int)	5505	3696	3423	4919
with $I > 2\sigma(I)$		1986		1329
params, restraints	0/648	2/234	0/318	318/537
largest δF peaks/e·Å^{-3}	0.417, −0.389	0.240, −0.320	0.589, −0.749	0.768, −0.602
R1 [$I > 2\sigma(I)$][a]	0.0537	0.0725	0.0824	0.150
wR2 (all reflns)[a]	0.1587	0.1758	0.1672	0.4804

[a] $R1 = \sum||F_o| - |F_c||/|F_o|$. $wR2 = [\sum w(F_o^2 - F_c^2)^2]/\sum[w(F_o^2)^2]^{1/2}$.

spectrum in DMSO-d_6: 10.0 (s, 2H), 9.04 (s, 2H), 8.54 (t, pyH, 1H), 8.19 (d, pyH 2H), 7.84 (d, PhH, 4H), 6.83 (d, PhH, 4H) ppm. Positive ion FAB mass spectrum: m/z 416 $(ZnL^2Cl)^+$. Infrared spectrum: ν_{O-H} = 3372.4 cm^{-1} (v br); $\nu_{C=N}$ = 1618.3 cm^{-1}. Molar conductance of 1.0 mM DMF solution (specific conductance = 4.8): Λ_M = 4.8 Ω^{-1} cm^2 mol^{-1} (nonelectrolyte). X-ray quality crystals were grown by slow diffusion of toluene into a DMSO solution of the complex.

Synthesis of Bis[2,6-pyridinedicarboxaldehydebis(*p*-hydroxyphenylimine)]nickel(II) Chloride, $Ni(L^2)_2Cl_2$. 2,6-Pyridinedicarboxaldehyde (1.00 g, 7.40 mmol) and 4-aminophenol (1.62 g, 14.8 mmol) were dissolved in 15 mL of absolute ethanol with stirring to give a yellow solution. $NiCl_2\cdot 6H_2O$ (0.890 g, 3.74 mmol) was dissolved in 10 mL of warm ethanol to give a green solution. Addition of the nickel(II) solution to that containing the ligand materials produced a color change to red-brown and gave a red-brown precipitate, which was collected on a Hirsch funnel by vacuum filtration. The brown microcrystalline powder was recrystallized in 84% yield with four DMSO molecules of solvation from hot DMSO/toluene, with crystals appearing upon slow cooling to room temperature. Positive ion FAB mass spectrometry: m/z 727 $(NiL^2_2Cl)^+$. Anal. Calcd for $C_{38}H_{30}Cl_2N_6NiO_4\cdot 4C_2H_6OS$: C, 51.31; H, 5.05; N, 7.80. Found: C, 51.19; H, 4.76; N, 8.00. Infrared spectrum: ν_{O-H} = 3154.9 cm^{-1}; $\nu_{C=N}$ = shoulder at approximately 1635 cm^{-1} in broad, multiply occupied 1600 cm^{-1} region. Cyclic voltammetry in methanol: $E_{1/2}$ = −1.053 V (ΔE_p = 65 mV) vs Fc/Fc$^+$. Uv/vis spectrum (2.9 × 10^{-2} mM in water scanning from 220 to 820 nm): 228 nm (ϵ = 4.4 × 10^4 cm^{-1} M^{-1}), 378 nm (ϵ = 2.3 × 10^4 cm^{-1} M^{-1}). Molar conductance of 0.714 mM aqueous solution (specific conductance = 127): Λ_M = 173 Ω^{-1} cm^2 mol^{-1}; Onsager plot,[24] slope = 325 (0.625 mM, λ = 107; 0.714 mM, λ = 121; 1.00 mM, λ = 165).

Anion Metathesis of $Ni(L^2)_2Cl_2$ To Give the Hexafluorophosphate, $Ni(L^2)_2(PF_6)_2$, and Triflate (Trifluoromethanesulfonate), $Ni(L^2)_2Tf_2$, Salts. The hexafluorophosphate salt was prepared by dissolving the chloride salt of the nickel(II) complex (0.5 g, 0.5 mmol) in ca. 20 mL of boiling water and filtering this solution into an aqueous solution containing excess ammonium hexafluorophosphate. The brown precipitate which appeared was collected by vacuum filtration, rinsed with cold water and diethyl ether, and then dried overnight in a vacuum desiccator. Recrystallization from hot acetonitrile/dichloroethane by slow evaporation of the solvents gave the pure compound in 64% yield. Anal. calcd for $C_{38}H_{30}F_{12}N_6NiO_4P_2$: C, 46.42; H, 3.08; N, 8.55. Found: C, 46.44; H, 3.15; N, 8.30. Positive ion FAB mass spectrometry: m/z 837 $(NiL^2_2PF_6)^+$. The triflate salt was prepared in a similar manner by adding 1.9 g of the chloride salt in hot water to an aqueous solution of excess sodium triflate. The crude triflate salt was recrystallized from boiling water to give the product in 87% yield. Anal. Calcd for $C_{40}H_{30}F_6N_6NiO_{10}S_2$: C, 48.46; H, 3.05; N, 8.48. Found: C, 48.76; H, 2.80; N, 8.70. Positive ion FAB mass spectrometry: m/z 841 $(NiL^2_2Tf)^+$.

The bromide salt of the cobalt(II) complex was prepared by the same method as illustrated above for $Ni(L^2)_2Cl_2$ using $CoBr_2\cdot 6H_2O$ in place of $NiCl_2\cdot 6H_2O$. Recrystallization of the crude product from hot DMSO/toluene gave the complex with five cocrystallized DMSO molecules in 75% overall yield. Anal. Calcd for $C_{38}H_{30}Br_2CoN_6O_4\cdot 5C_2H_6OS$: C, 46.34; H, 4.86; N, 6.76. Found: C, 46.14; H, 4.86; N, 7.00. Positive ion FAB mass spectrometry: m/z 774 $(CoL^2_2Br)^+$.

Methylation of $Ni(L^2)_2(PF_6)_2$. The nickel(II) complex (0.510 g, 0.519 mmol) and anhydrous potassium carbonate (2.08 g, 15.0 mmol) were stirred in 50 mL of dry acetonitrile (distilled over calcium hydride). Methyl iodide (0.630 g, 4.43 mmol) was added, and the mixture was protected from light and heated at 55 °C for 24 h. The mixture was filtered, and solvent was removed from the red-brown solution to give a brown, grainy product. Recrystallization from acetonitrile/ethanol by slow evaporation of the solvents gave red-brown crystals with impurities of clear, thin sheets which could not be removed, even with additional recrystallizations from acetonitrile/ethanol or acetonitrile/ethanol/water or by rinsing with various organic solvents or with water. The product was analyzed by mass spectrometry, and the structure of the red-brown crystals was solved by X-ray crystallography. Positive ion FAB mass spectrum: m/z 748 $[Ni(LMe_2)_2(PF_6)_2]^+$.

Benzylation of $Ni(L^2)_2(PF_6)_2$. The nickel(II) complex (0.495 g, 0.503 mmol), benzyl bromide (0.72 g, 4.2 mmol), and anhydrous potassium carbonate (0.504 g, 3.65 mmol) were stirred in 35 mL of dry acetonitrile at room temperature for 24 h. The mixture was filtered, and solvent was removed from the red-brown solution by rotary evaporation. The crude product was dissolved in ca. 10 mL of acetonitrile to which an ethanolic solution of excess ammonium hexafluorophosphate was added. A brown product precipitated after a few hours and was collected and rinsed with ethanol and diethyl ether. This salt was recrystallized from acetonitrile/ethanol by slow evaporation of the solvents to give small, brown needles in 27% yield. Anal. calcd for $C_{66}H_{54}F_{12}N_6NiO_4P_2$: C, 58.99; H, 4.05; N, 6.25. Found: C, 58.59; H,4.10; N, 6.00. Positive ion FAB mass spectrum: m/z 1052 $[Ni(LBz_2)_2(PF_6)_2]^+$.

Crystal Structure Analysis. Summary crystal data is given in Table 3, and full crystallographic details and tables are included in the Supporting Information. Data for the first and fourth compounds was taken on a conventional Siemens four-circle diffractometer in $\omega-2\theta$ mode, and for the others was taken on a Siemens CCD area detector. Most of the crystals diffracted rather poorly, with a rapid falloff in

intensity, generally leading to rather high *R* values. This was particularly true of $Ni(L^2)_2Cl_2$, which formed extremely thin plates that formed disorientated aggregates. However, despite the very poor conventional *R* value, the structure was successfully refined to give a clear picture of the molecule. The asymmetric unit of $Ni(Me\text{-}L^2)_2Cl_2$ contains one full molecule and two half-molecules, the latter both lying on 2-fold axes; these molecules are structurally identical. These crystals also suffered from twinning problems, and several crystals had to be examined before one could be found for which one component was dominant.

Acknowledgment. A.L.V. thanks the Madison and Lila Self Graduate Fellowship Program of The University of Kansas for financial support. This material is based upon work supported by the NSF under Grant 9550487 and matching support from the state of Kansas. The support of EPSRC and Siemens Analytical Instruments for the purchase of the SMART system is gratefully acknowledged. The Warwick−Kansas collaboration has been supported by NATO.

Supporting Information Available: Text describing X-ray structural analysis, and tables containing final atomic coordinates, H-atom coordinates, thermal parameters and bond lengths and angles, and X-ray crystallographic files for the structure determination for $Zn(L^1)_2(PF_6)_2$, $Zn(L^2)_2(Cl)_2$, and $Ni(L^2)_2(Cl)_2$ (73 pages). Corresponding data in CIF format for the ligand L^2 and $Ni(MeL^2)_2(PF_6)_2$ are available on the Internet only. Ordering and access information is given on any current masthead page.

IC9714201